

**SYNTHESIS AND CHARACTERIZATION OF THERMALLY STABLE
POLY(AMIDE-IMIDE)-MONTMORILLONITE NANOCOMPOSITES
BASED ON BIS(4-CARBOXYPHENYL)-N,N'-PYROMELLITIMIDE ACID**

Khalil Faghihi^{1*}, Ali Asghari² and Mohsen Hajibeygi³

¹Department of Chemistry, Faculty of Science, Arak University, Arak, 38156-8-8349, Iran

²Department of Chemistry, Arak Branch, Islamic Azad University, Arak, Iran

³Department of Chemistry, Varamin Pishva Branch, Islamic Azad University, Varamin, Iran

(Received May 10, 2011; revised November 28, 2012)

ABSTRACT. Two new poly(amide-imide)-montmorillonite reinforced nanocomposites containing bis(4-carboxyphenyl)-N,N'-pyromellitimide acid moiety in the main chain were synthesized by a convenient solution intercalation technique. Poly(amide-imide) (PAI) as a source of polymer matrix was synthesized by the direct polycondensation reaction of bis(4-carboxyphenyl)-N,N'-pyromellitimide acid with 4,4'-diamino diphenyl sulfone in the presence of triphenyl phosphite (TPP), CaCl₂, pyridine and N-methyl-2-pyrrolidone (NMP). Morphology and structure of the resulting PAI-nanocomposite films with 10 and 20% silicate particles were characterized by FT-IR spectroscopy, X-ray diffraction (XRD) and scanning electron microscopy (SEM). The effect of clay dispersion and the interaction between clay and polymeric chains on the properties of nanocomposites films were investigated by using UV-Vis spectroscopy, thermal gravimetry analysis (TGA) and water uptake measurements.

KEYWORDS: Bis(4-carboxyphenyl)-N,N'-pyromellitimide acid moiety, Poly(amide-imide)-montmorillonite nanocomposite, Thermal properties

INTRODUCTION

Polymer-clay nanocomposites typically exhibited mechanical, thermal and gas barrier properties, which are superior to those of the corresponding pure polymers [1-9]. Unique properties of the nanocomposites are usually observed when the ultra fine silicate layers are homogeneously dispersed throughout the polymer matrix at nanoscale. The uniform dispersion of silicate layers is usually desirable for maximum reinforcement of the materials. Due to the incompatibility of hydrophilic layered silicates and hydrophobic polymer matrix, the individual nanolayers are not easily separated and dispersed in many polymers. For this purpose, silicate layers are usually modified with an intercalating agent to obtain organically modified clay prior to use in nanocomposite formation [10, 11]. Also aromatic polyimides are well recognized as a class of high performance materials due to their remarkable thermal and oxidative stabilities and excellent electrical and mechanical properties for long time periods of operation [12]. Unfortunately, strong interaction between polyimide chains and their rigid structure make them intractable. Poor thermoplastic fluidity and solubility are the major problems for wide application of polyimides. Thus, to overcome these processing problems various approaches have been carried out by incorporating flexible units such as -NHCO-, -O-, and -SO₂-, and some of which are commercialized [13-14]. Among them, poly(amide-imide) (PAI) is the most successful material, which combines the advantages of high-temperature stability and processability [15-22]. In this article two PAI-nanocomposite films with 10 and 20% silicate particles containing chiral bis(4-carboxyphenyl)-N,N'-pyromellitimide acid moiety in the main chain was prepared by using a convenient solution intercalation technique.

*Corresponding author. E-mail: k-faghihi@araku.ac.ir

EXPERIMENTAL

Materials

Pyromellitic dianhydride, *p*-amino benzoic acid, 4,4'-diamino diphenyl sulfone, acetic acid, triphenyl phosphite (TPP), CaCl₂, pyridine and N-methyl-2-pyrrolidone (NMP), N,N-dimethyl formamide (DMF) were purchased from Merck Chemical Company and used without previous purification. Purified the organically-modified Cloisite® 20A supplied by Southern Clay Products (TX), were used as polymer nanoreinforcement.

Measurements

¹H-NMR spectra was recorded on a Bruker 300 MHz instrument (Germany). Fourier transform infrared (FT-IR) spectra were recorded on Galaxy Series FT-IR 5000 spectrophotometer (England). UV-Vis spectra were recorded at 25 °C in the 300-800 nm spectral regions with a Perkin Elmer Lambda 15 spectrophotometer in NMP solution using cell lengths of 1 cm. Thermogravimetric analysis and differential scanning calorimetry (TGA and DSC) data were taken on a Mettler TA4000 System under N₂ atmosphere at a rate of 10 °C/min. The morphology and structure of nanocomposite film was investigated on Cambridge S260 scanning electron microscope (SEM) and Rigaku D - max CIII X-ray diffraction (XRD). Elemental analyses were taken on a Vario AV.

Monomer synthesis

A mixture of pyromellitic dianhydride **1** (3.00 g, 13.70 mmol), *p*-amino benzoic acid **2** (3.76 g, 27.50 mmol) and 130 mL acetic acid with appropriate amounts of pyridine was stirred and mixture was refluxed at 120 °C for 12 h until the precipitate was formed, the precipitate was filtered off, washed thoroughly with water and dried to afford 4.52 g compound **3** (yield 72.1%). M.p.: 310 °C, FT-IR (KBr): 3500-2500, 3070, 1778, 1722, 1600-1580, 1422-1370, 1277, 922, 709 cm⁻¹. ¹H-NMR (DMSO-d₆) δ: 7.42-8.12 (10H, aromatic), 13.15 (2H, OH) ppm.

Polymer synthesis

Into a 100 mL round bottomed flask were placed a mixture of N-pyrromellitimido-4-amino benzoic acid **3** (0.72 g, 1.57 mmol), 4,4'-diamino diphenyl sulfone **4** (0.39 g, 1.57 mmol), calcium chloride (0.60 g), triphenyl phosphite (1.00 mL), pyridine (1.00 mL) and N-methyl-2-pyrrolidone (4.00 mL). The mixture was heated for 1 h at 60 °C, 2 h at 90 °C and then refluxed at 140 °C for 9 h until a viscous solution was formed. Then it was cooled to room temperature and 30 mL of methanol was added to reaction mixture. The precipitate was formed, filtered off and washed with methanol. The resulting polymers **5** were dried under vacuum to leave 0.93 g (90%). FT-IR (KBr): 3415, 3190-3065, 1774, 1718, 1664, 1587, 1503, 1369, 1318, 1144, 1101, 708 cm⁻¹. Elemental analysis for C₃₆H₂₀N₄O₈S, calculated; C, 64.7; H, 3.0; N, 8.4; found; C, 65.5, H, 3.0; N, 9.1.

PAI-nanocomposite synthesis **5a** and **5b**

PAI-nanocomposites **5a** and **5b** were produced by solution intercalation method, in two different amounts of organoclay particles (10 and 20 wt.%) were mixed with appropriate amounts of PAI (0.50 g, 0.74 mmol) solution in NMP (8.00 mL) to yield particular nanocomposite concentrations. To control the dispersibility of organoclay in PAI matrix,

constant stirring was applied at 25 °C for 24 h. Nanocomposite films were cast by pouring the solutions for each concentration into Petri dishes placed on a labelled surface followed by the evaporation of solvent at 70 °C for 12 h. Films were dried at 80 °C under vacuum to a constant weight. FT-IR(KBr) for PAI-nanocomposites **5a**: 3435, 3190, 1775, 1719, 1660, 1587, 1503, 1369, 1318, 1144, 1100, 1041, 754, 511 cm⁻¹. FT-IR (KBr) for PAI-nanocomposites **5b**: 3440, 3165-3045, 1775, 1720, 1661, 1587, 1503, 1369, 1318, 1145, 1101, 1042, 753, 458 cm⁻¹.

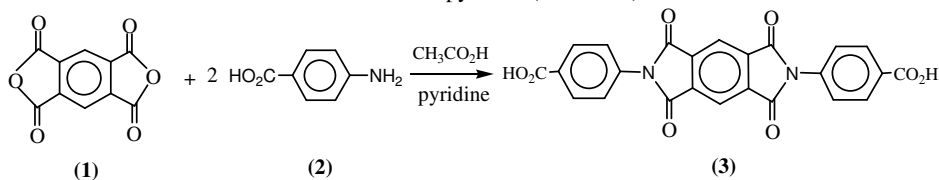
The water absorption analysis

The water absorption of PAI-nanocomposite films was carried out using a procedure under ASTM D570-81 [24]. The films were dried in a vacuum oven at 80 °C to a constant weight and then weighed to get the initial weight (W_0). The dried films were immersed in deionized water at 25 °C. After 24 h, the films were removed from water and then they were quickly placed between sheets of filter paper to remove the excess water and films were weighed immediately. The films were again soaked in water. After another 24 h soaking period, the films were taken out, dried and weighed for any weight gain. This process was repeated again and again till the films almost attained the constant weight. The total soaking time was 168 h and the samples were weighed at regular 24 h time intervals to get the final weight (W_f). The percent increase in weight of the samples was calculated by using the formula $(W_f - W_0)/W_0$.

RESULTS AND DISCUSSION

Monomer synthesis

bis(4-Carboxyphenyl)-N,N'-pyromellitimide acid **3** was synthesized by the condensation reaction of one equimolar of pyromellitic dianhydride **1** with two equimolar of *p*-amino benzoic acid **2** in a mixture of acetic acid solution and pyridine (Scheme 1).



Scheme 1. Synthetic route of bis(4-carboxyphenyl)-N,N'-pyromellitimide acid **3**.

The chemical structure of diacid **3** was confirmed by FT-IR and ¹H-NMR spectroscopy. In the FT-IR spectrum of diacid **3** peaks appearing at 3500-2500 cm⁻¹ (acid O-H stretching), 1778 cm⁻¹ (C=O asymmetric imide stretching), 1722 cm⁻¹ (C=O acid and symmetric imide stretching), 1422-1370 and 709 cm⁻¹ (imide characteristic ring vibration) confirmed the presence of imide ring and carboxylic groups in this compound (Figure 1). The ¹H-NMR spectrum of diacid **3** shows peaks between $\delta = 7.42$ -8.12 ppm related to aromatic protons and a broad peak at $\delta = 13.15$ ppm was assigned for protons of the COOH groups (Figure 2).

Polymer synthesis

PAI **5** was synthesized by the direct solution polycondensation reaction of an equimolar mixture of diacid **3**, an equimolar mixture of diamine **4** with triphenyl phosphite, NMP, calcium chloride and pyridine as condensing agents (Scheme 2).

The entire polycondensation readily proceeded in a homogeneous solution. Tough and stringy precipitate formed when the viscous PAI solution was obtained in good yield (90%).

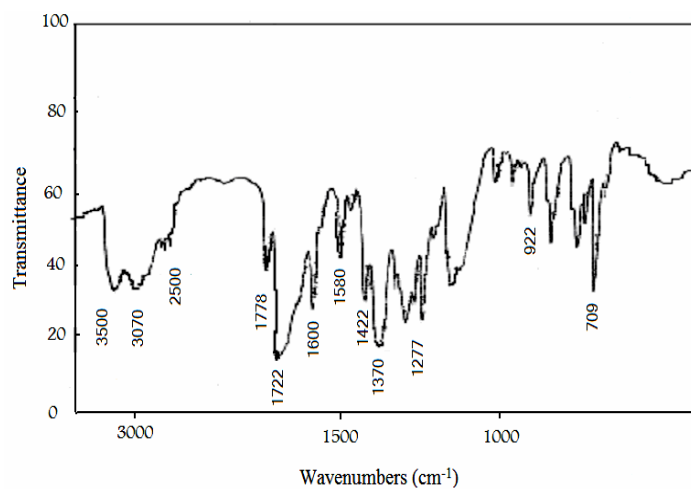


Figure 1. FT-IR spectrum of diacid 3.

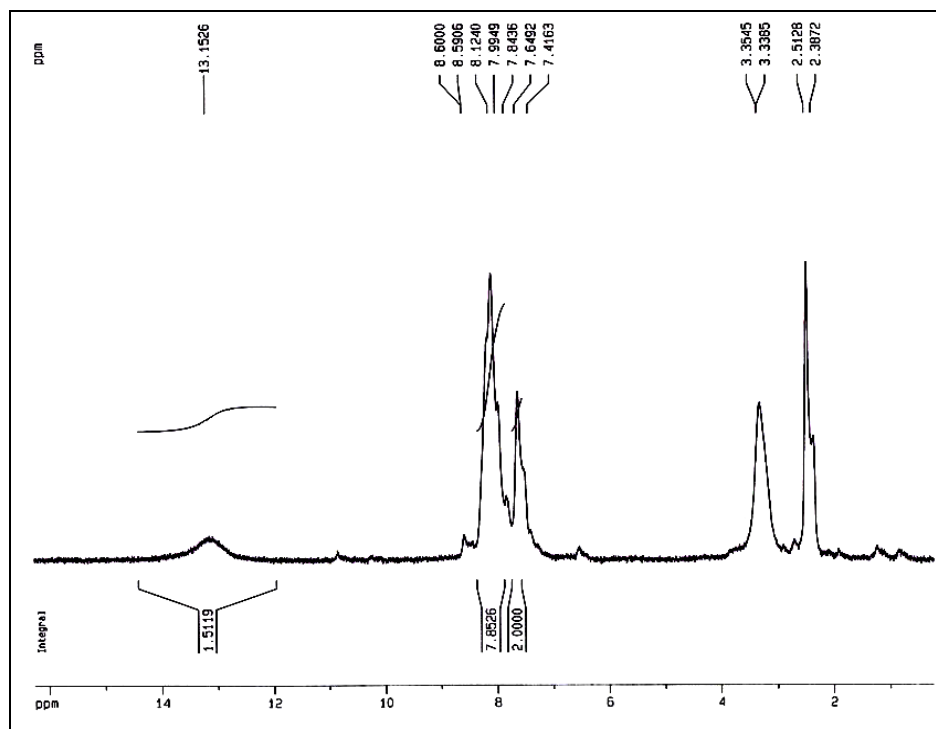
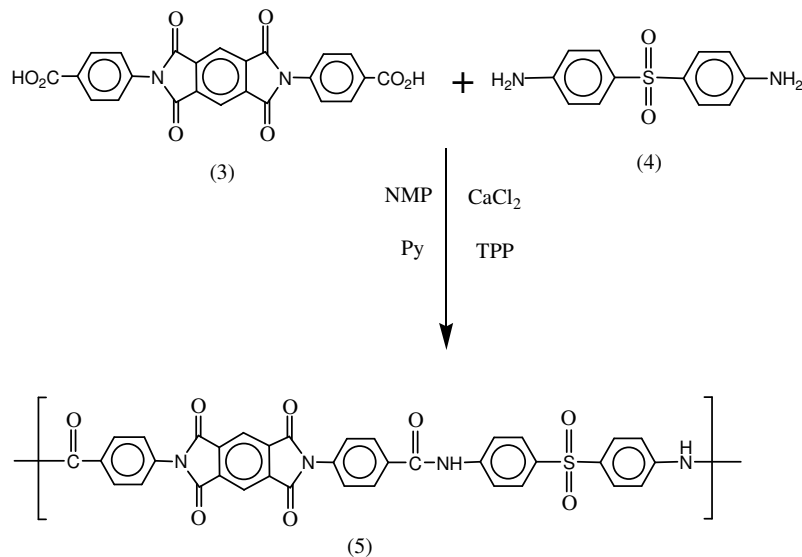


Figure 2. ¹H-NMR spectrum of diacid 3.

Scheme 2. Synthetic route of poly(amide-imide) **5**.

Polymer characterization

This polymer had inherent viscosity of 0.29 dL/g (Measured at a concentration of 0.5 g dL⁻¹ in DMF at 25 °C) and was confirmed as PAI by using FT-IR spectroscopy and elemental analysis. A representative FT-IR spectrum of PAI **5** is shown in (Figure 3). PAI **5** had absorption bands between 1774 cm⁻¹ and 1664 cm⁻¹ due to imide and amide carbonyl groups. Absorption bands around 1369-1318 cm⁻¹ and 732 cm⁻¹ demonstrated the presence of the imide heterocyclic ring in this polymer. Also absorption band of amide group appeared at 3415 cm⁻¹ (N-H stretching). The elemental analysis value of the resulting polymer was in good agreement with the calculated values for the proposed structure.

The solubility of PAI **5** was investigated with 0.01 g polymeric sample in 2 mL of solvent. PAI (**5**) was dissolved in organic solvent such as DMF, DMSO and NMP at room temperature and it was insoluble in solvents such as chloroform, methylene chloride, methanol, ethanol and water.

PAI-nanocomposite films

PAI-nanocomposite films were transparent and yellowish brown in color. The incorporation of organoclay changed the color of films to dark yellowish brown. Moreover, a decrease in the transparency was observed at higher clay contents. (Scheme 3) show the flow sheet diagram and synthetic scheme for PAI-nanocomposite films **5a** and **5b**.

The chemical structure of PAI-nanocomposite films **5a** and **5b** were determined by using FT-IR, X-ray diffraction (XRD) and Scanning electron microscopy (SEM) techniques.

FT-IR spectra of PAI-nanocomposite films **5a** and **5b** showed the characteristic absorption bands of the Si-O and Mg-O moieties at 1041, 511 and 465 cm⁻¹, respectively. The incorporation of organic groups in PAI-nanocomposite films were confirmed by the presence of peaks at 1775, 1719, 1369, 754 (imide rings) and 1660, 1318 (amide groups) (Figure 4).

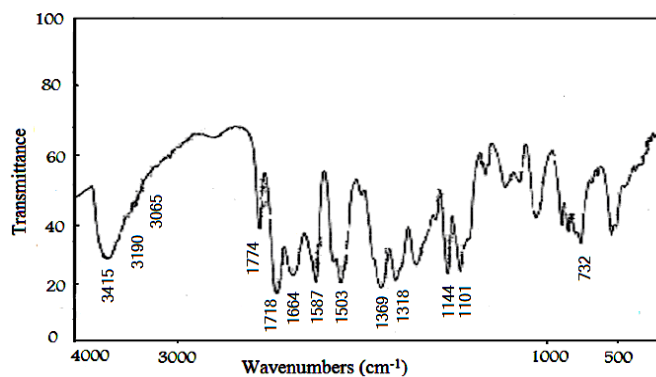
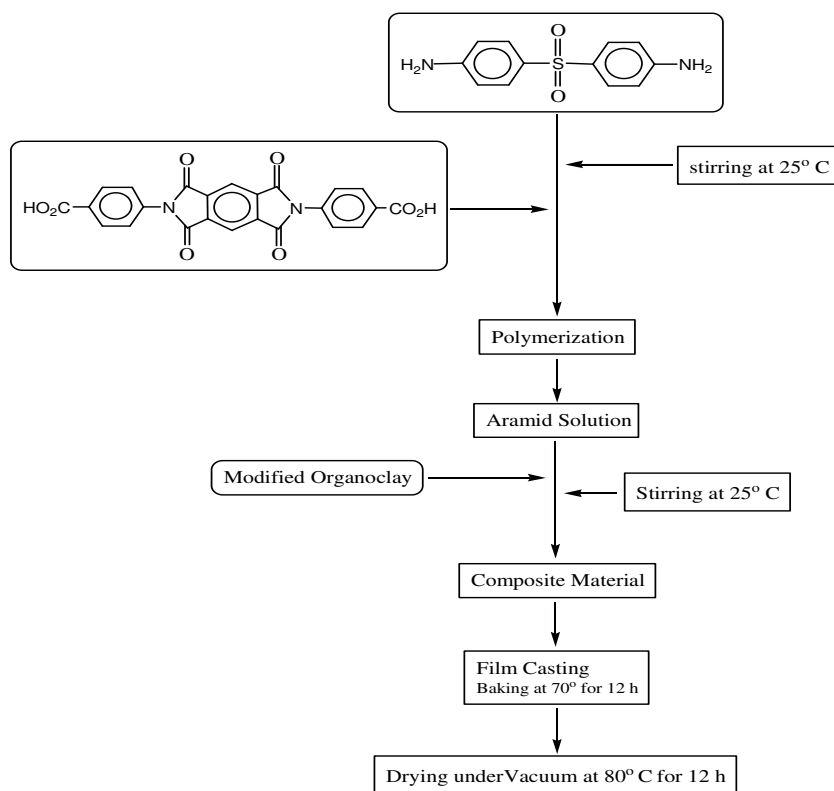


Figure 3. FT-IR spectrum of PAI 5.

Scheme 3. Flow sheet diagram for the synthesis of PAI-nanocomposites film **5a** and **5b**.

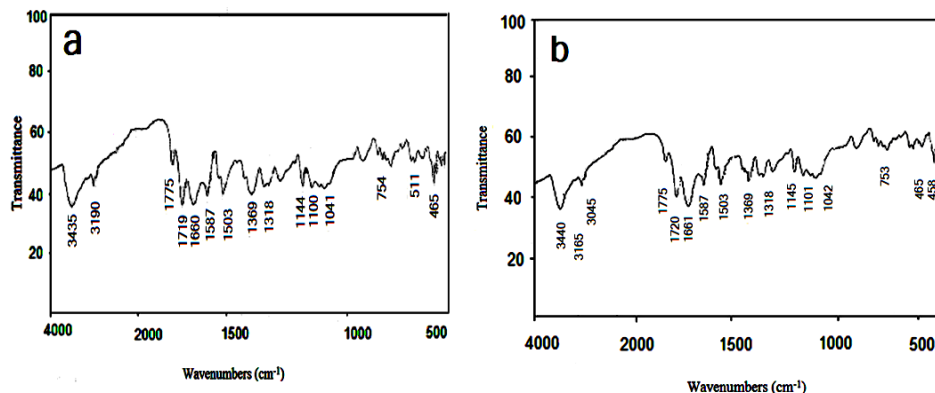


Figure 4. FTIR spectra of PAI-nanocomposite films **5a** (a) and **5b** (b).

Figure 5 shows the XRD patterns of PAI-nanocomposite films **5a** and **5b** containing 10 and 20 wt.% of silicate particles. The result reveals an increased d-spacing from 1.00 nm (8.93°) of Na-MMT to 1.49 nm (5.15°) of PAI-nanocomposite film (10 wt.%) and (4.23 $^\circ$) of PAI-nanocomposite film (20 wt.%). These results indicated significant expansion of the silicate layer after insertion to PAI chains. The shift in the diffraction peaks PAI-nanocomposite films confirms that intercalation has been taken place. This is direct evidence that PAI-nanocomposites have been formed as the nature of intercalating agent also affects the organoclay dispersion in the polymer matrix. Usually there are two types of nanocomposites depending upon the dispersion of clay particles. The first type is an intercalated polymer clay nanocomposite, which consists of well ordered multi layers of polymer chain and silicate layers a few nanometers thick. The second type is an exfoliated polymer-clay nanocomposite, in which there is a loss of ordered structures due to the extensive penetration of polymer chain into the layer silicate. Such part would not produce distinct peaks in the XRD pattern [25]. In our PAI-nanocomposite films there are coherent XRD signal at 5.15° and 4.23° related to 10 and 20 wt.% nanocomposite films, respectively.

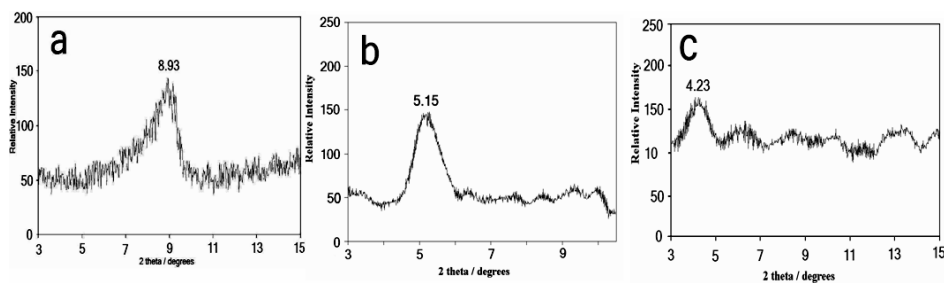


Figure 5. X-ray diffraction patterns of organoclay (a), PAI-nanocomposite films **5a** (b) and **5b** (c).

The surface morphology of the PAI-nanocomposite films prepared by solution intercalation technique is compared by SEM analyses. (Figure 6) show the morphological images of 10 and 20 wt.% nanocomposite films, respectively. The SEM images show that PAI matrix has a smooth morphology, whereas the PAI matrix has an amorphous morphology. Also SEM micrographs of PAI-nanocomposite containing 10 and 20 wt.% clay platelets were uniformly distributed without agglomeration.

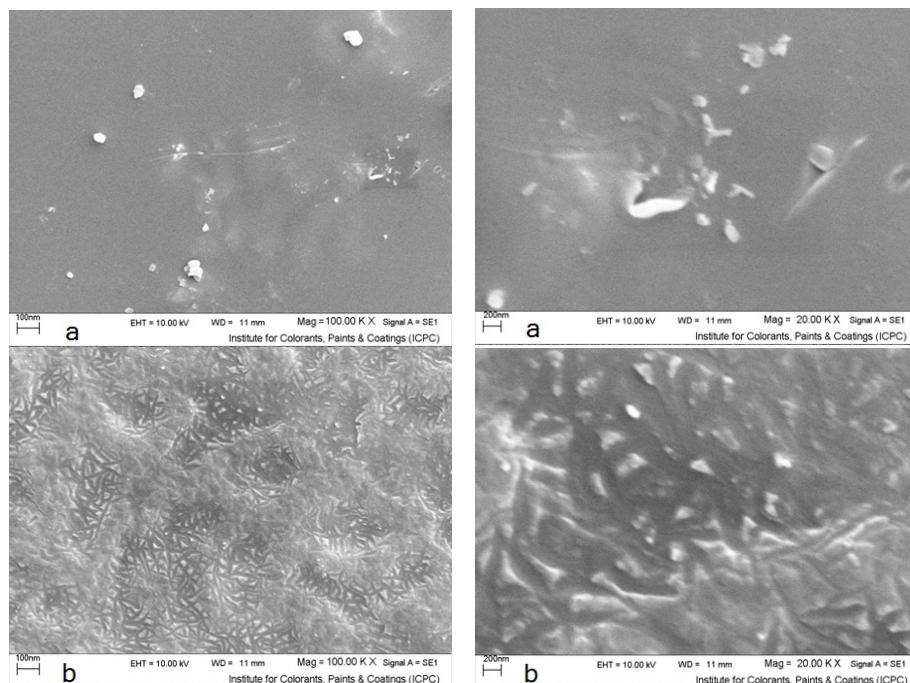


Figure 6. Scanning electron micrographs of PAI-nanocomposite films **5a** (a) and **5b** (b).

Comparing of thermal gravimetry analysis, optical clarity and water absorption between PAI and PAI-nanocomposite films

Optical clarity

Optical clarity of PAI-nanocomposite films containing 10 and 20 wt.% clay platelets and neat PAI were compared by UV-Vis spectroscopy in the region of 300-800 nm. (Figure 7) show the UV-Vis transmission spectrum of pure PAI and PAI-nanocomposite films containing 10 and 20 wt.% clay platelets. This spectrum show that the UV-Vis region (300-800 nm) is affected by the presence of the clay particles and exhibiting low transparency reflected to the primarily intercalated composites. Results show that the optical clarity of PAI-nanocomposite films system is significantly lower than the neat PAI system.

Thermal gravimetry analysis

The thermal properties of PAI-nanocomposite films containing 10 and 20 wt.% clay platelets and neat PAI were investigated by using TGA and DSC in nitrogen atmosphere at a rate of heating of 10 °C/min, and thermal data are summarized in (Table 2). These samples exhibited good resistance to thermal decomposition, up to 145-180 °C in nitrogen, and began to decompose gradually above this temperature. T_5 for these samples ranged from 145-180 °C and T_{10} for them ranged from 175-220 °C, and residual weights at 600 °C ranged from 50.07-55.72% in nitrogen. Incorporation of organoclay into the PAI matrix also enhanced the thermal stability of the nanocomposites. Figure 8 shows the TGA thermograms of PAI-nanocomposites

under nitrogen atmosphere. Thus, we can speculate that interacting PAI chains between the clay layers serve to improve the thermal stability of nanocomposites. The addition of organoclay in polymeric matrix can significantly improve the thermal stability of PAI.

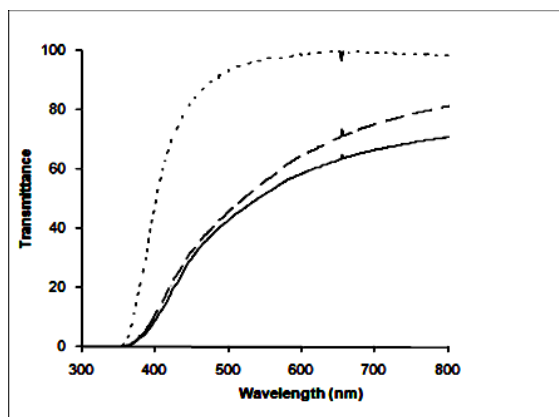


Figure 7. UV-Vis spectrum of PAI **5** ·····, PAI-nanocomposite films **5a** - - - and **5b** — — .

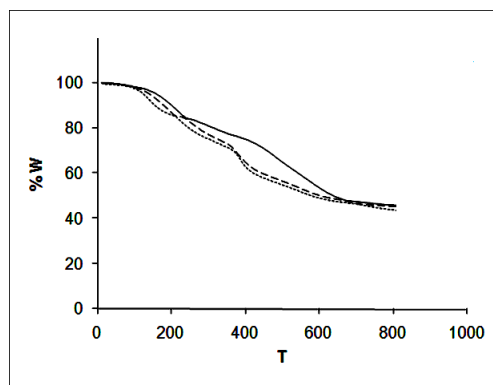


Figure 8. TGA spectrum of PAI **5** ·····, PAI-nanocomposite films **5a** - - - and **5b** — — .

Water absorption

The PAI under investigation contains polar and cyclic imide rings and also polar amide groups in the backbone that have the tendency to uptake water through hydrogen bonding. Thus water absorption measurements become necessary for neat PAI **5** and PAI-nanocomposite films **5a** and **5b** and data are shown in (Table 1). In the water permeability studies, we found that the incorporation of clay platelets into PAI matrix results in a decrease of water uptake relative to pure PAI by forming the tortuous path of water permeant. Water permeability depends on length, orientation and degree of delamination of layered silicate. It should be noted that a further increase in clay concentration resulted in an enhanced barrier property of nanocomposites which may be attributed to the plate-like clays that effectively increase the length of the diffusion pathways, as well as decrease the water permeability.

Table 1. Thermal behaviors and water uptake of neat PAI (**5**) and PAI-nanocomposite films **5a** and **5b**.

Sample	T ₅ (°C) ^a	T ₁₀ (°C) ^b	Char Yield ^c	Water uptake (%) ^d
5	144	174	50.0	4.17
5a	160	198	51.3	1.81
5b	179	220	55.7	0.22

^{a,b}Temperature at which 5% and 10% weight loss was recorded by TGA at heating rate of 10 °C/min in N₂, respectively ^dPercentage weight of material left undecomposed after TGA analysis 800 °C.

CONCLUSION

The PAI-nanocomposites were successfully prepared using solution intercalation method. The structure and the uniform dispersion of organoclay throughout the PAI matrix were confirmed by FT-IR, XRD and SEM analyses. The optical clarity and water absorption property of PAI-nanocomposites were decreased significantly with increasing the organoclay contents in PAI matrix. On the contrary the thermal stability of PAI-nanocomposites were increased significantly with increasing the organoclay contents in PAI matrix. The enhancements in the thermal stability of the nanocomposites films **5a** and **5b** by introducing organoclay may be due to the strong interactions between polymeric matrix and organoclay, as well as intercalation and dispersion of clay platelets in the PAI matrix.

REFERENCES

1. Giannelis, E.P. *Adv. Mater.* **1996**, 8, 29.
2. Yano, Y.; Usuki, A.; Kurauchi, T.; Kamigato, O. *J. Polym. Sci. Part A: Polym. Chem.* **1993**, 31, 2493.
3. Zulfiqar, S.; Ahmad, Z.; Ishhagh, M.; Saeed, S.; Sarwar, M.I. *J. Mater. Sci.* **2007**, 42, 93.
4. Sikka, M.; Cerini, L.N.; Ghosh, S.S.; Wieny, K.I. *J. Polym. Sci. Part B: Polym. Phys.* **1996**, 34, 1443.
5. Xu, R.; Manias, E.; Snyder, A. J.; Runt, J. *Macromolecules* **2001**, 34, 337.
6. Kausar, A.; Zulfiqar, S.; Shabbir, S.; Ishhagh, M.; Sarwar, M.I. *Polym. Bull.* **2007**, 59, 457.
7. Bibi, N.; Sarwar, M.I.; Ishhagh, M.; Ahmad, Z. *Polym. Polym. Compos.* **2007**, 15, 313.
8. Zulfiqar, S.; Sarwar, M. I. *Scr. Mater.* **2008**, 59, 436.
9. Fornes, T.D.; Yoon, P.J.; Hunter, D.L.; Keskkula, H.; Paul, D.R. *Polymer* **2002**, 43, 5915.
10. Chen, G.M.; Ma, Y.M.; Qi, Z.N. *J. Appl. Polym. Sci.* **2000**, 77, 2201.
11. Yano, Y.; Usukia, A.; Kurauchi, T.; Kamigato, O. *J. Polym. Sci. Part A: Polym. Chem.* **1993**, 31, 2493.
12. Ghosh, M. K.; Mittal, K.L. *Polyimide: Fundamental and Applications*, Dekker: New York; **1996**.
13. Liaw, D.J.; Liaw, B.Y.; *Polymer* **2001**, 42, 839.
14. Zhang, Q.; Li, S.; Li, W.; Zhang, S. *Polymer* **2007**, 48, 6246.
15. Zhang, Q.; Chen, S. *Polymer* **2007**, 48, 2250.
16. Saxena, A.; Rao, V.L.; Prabhakaran, P.V.; Nianan, K.N. *Eur. Polym. J.* **2003**, 39, 401.
17. Yang, C.P.; Chen, Y.P.; Woo, E.M. *Polymer* **2004**, 45, 5279.
18. Liaw, D.J.; Chen, W.H. *Polym. Degrad. Stab.* **2006**, 91, 1731.
19. Mallakpour, S.; Kolahdoozan, M. *J. Appl. Polym. Sci.* **2007**, 104, 1248.
20. Faghihi, Kh.; Naghavi, H. *J. Appl. Polym. Sci.* **2005**, 96, 1776.
21. Faghihi, Kh.; Mozafari, Z. *Turk. J. Chem.* **2008**, 32, 673.
22. Mallakpour, S.; Hajipour, A.R.; Habibi, S. *J. Appl. Polym. Sci.* **2001**, 80, 1312.
23. Zulfiqar, S.; Sarwar, M.I. *J. Incl. Phenom. Macrocycl. Chem.* **2008**, 62, 353.
24. Krishnan, P.S.G.; Wisanto, A.E.; Osiyemi, S.; Ling, C. *Polym. Inter.* **2007**, 56, 787.
25. Bharadwaj, R.K. *Macromolecules* **2001**, 34, 9189.